Exactly soluble model for nuclear liquid-gas phase transition

K. A. Bugaev,[1,2] M. I. Gorenstein,[1,2] I. N. Mishustin,[1,3,4] and W. Greiner[1]
[1]*Institut für Theoretische Physik, Universität Frankfurt, Frankfurt, Germany*
[2]*Bogolyubov Institute for Theoretical Physics, Kyiv, Ukraine*
[3]*The Kurchatov Institute, Russian Research Center, Moscow, Russia*
[4]*The Niels Bohr Institute, University of Copenhagen, Copenhagen, Denmark*
(Received 8 June 2000; published 20 September 2000)

Thermodynamical properties of nuclear matter undergoing multifragmentation are studied within a simplified version of the statistical model. An exact analytical solution has been found for the grand canonical ensemble. Excluded volume effects are taken into account in the thermodynamically self-consistent way. In the thermodynamic limit the model exhibits a first order liquid-gas phase transition with specific mixed phase properties. An extension of the model including the Fisher's term is also studied. The possibility of the second order phase transition at or above the critical point is demonstrated. The fragment mass distributions in different regions of the phase diagram are discussed.

PACS number(s): 21.65.+f, 24.10.Pa, 25.70.Pq

I. INTRODUCTION

Nuclear multifragmentation, i.e., multiple production of intermediate mass fragments, is one of the most spectacular phenomena in intermediate energy nuclear reactions. The statistical multifragmentation model (SMM) has been developed during the past two decades (see [1,2] and references therein). Numerous comparisons with experimental data (see, e.g., Refs. [3,4]) show that it is rather successful in explaining many important features of nuclear multifragmentation. Moreover, there are serious indications [4,5] that multifragmentation in equilibrated systems is related to a liquid-gas phase transition in nuclear matter. Recently a simplified version of the SMM has been proposed [6,7] to study this relationship. The calculations within the canonical ensemble of noninteracting fragments suggest the existence of a first order phase transition. This was demonstrated by increasing the total number of particles in the system up to $A=2800$. These numerical calculations appeared to be rather efficient due to the recursive formula [8] which explicitly expressed the canonical partition function for A particles in terms of the canonical partition functions for $1,2,\ldots,A$-1 particles. The recursive procedure essentially simplifies the numerical evaluations and makes them possible for rather large values of A. However, the analytical studies of the system behavior in the thermodynamic limit, i.e., when both the system mass number A and volume V go to infinity, are still missing. On the other hand, the investigation of the thermodynamic limit is crucial to proof the existence of a phase transition and to study its exact nature.

In the present paper we give an exact analytical solution of the simplified version of the SMM performing its complete study in the thermodynamic limit. The accurate treatment of the excluded volume effects is an important part of our study. We work in the grand canonical ensemble which significantly simplifies the mathematical problems and leads to the explicit analytical solution in the thermodynamic limit.

The paper is organized as follows. In Sec. II the simplified version of the SMM is formulated. In Sec. III we introduce the isobaric partition function. The relationship between its singularities and the phase transition existence is discussed in Sec. IV. Section V deals with the first order phase transition and properties of the mixed phase. In Sec. VI the possibility of a second order phase transition is demonstrated. Fragment mass distributions are discussed in Sec. VII. Section VIII is reserved for conclusions.

II. MODEL FORMULATION

Let us consider a system composed of many different nuclear fragments and characterized by the total number of nucleons A, volume V and temperature T. The system states are specified by the multiplicities $\{n_k\}$ $(n_k=0,1,2,\ldots)$ of k-nucleon fragments $(k=1,2,\ldots,A)$. The partition function of a single fragment with k nucleons is assumed to have the standard form [1] (here and below the units $\hbar=c=1$ are used)

$$\omega_k = V\left(\frac{mTk}{2\pi}\right)^{3/2} z_k, \tag{1}$$

where m is the nucleon mass and the fragment mass is approximated as mk. The first two factors in Eq. (1) originate from the nonrelativistic thermal motion of the k fragment in the volume V at temperature T. The last factor, z_k, represents the intrinsic partition function of the k fragment. For $k=1$ (nucleon) we take $z_1=4$ (four internal spin-isospin states) and for fragments with $k>1$ we use the expression motivated by the liquid drop model (see details in Ref. [1]):

$$z_k = \exp\left(-\frac{f_k}{T}\right), \tag{2}$$

where

$$f_k = \sigma(T)k^{2/3} - [W_0 + T^2/\epsilon_0]k + \tau T\ln(k) \tag{3}$$

is the internal free energy of the k fragment. Here $W_0=16$ MeV is the volume binding energy per nucleon, T^2/ϵ_0 is the contribution of the excited states taken in the Fermi-gas ap-

proximation ($\epsilon_o = 16$ MeV), and $\sigma(T)$ is the surface free energy tension which is parametrized in the following form:

$$\sigma(T) = \sigma_o \left(\frac{T_c^2 - T^2}{T_c^2 + T^2} \right)^{5/4} \theta(T_c - T), \tag{4}$$

with $\sigma_o = 18$ MeV and $T_c = 18$ MeV. Finally, $\tau T \ln(k)$ is the phenomenological Fisher's term [9] (τ is a dimensionless constant) which we introduce to generalize our discussion. This form of z_k (with $\tau = 0$) was used in Refs. [6,7]. The symmetry and Coulomb contributions to the free energy are neglected. Such a model, however, appears to be a good starting point for the phase transition studies.

III. ISOBARIC PARTITION FUNCTION

The canonical partition function (CPF) of the ideal gas of nuclear fragments has the following form:

$$Z_A(V,T) = \sum_{\{n_k\}} \prod_k \frac{\omega_k^{n_k}}{n_k!} \delta\left(A - \sum_k k n_k \right), \tag{5}$$

where δ function takes care of the total baryon number conservation. An important assumption of the model is that the fragments do not overlap in a coordinate space. This gives rise to the repulsive interaction which we take into account in the Van der Waals excluded volume approximation. This is achieved by substituting the total volume V in Eq. (5) by the free volume $V_f \equiv V - bA$, where $b = 1/\rho_o$ ($\rho_o = 0.16$ fm^{-3} is the normal nuclear density). The calculation of the CPF (5) is difficult because of the restriction $\Sigma_k k n_k = A$. This constraint can be avoided by calculating the grand canonical partition function (GCPF). Using the standard definition we can write

$$\begin{aligned} \mathcal{Z}(V,T,\mu) &\equiv \sum_{A=0}^{\infty} e^{\mu A/T} Z_A(V - bA, T) \Theta(V - bA) \\ &= \sum_{\{n_k\}} \prod_k \frac{1}{n_k!} \left[\left(V - b \sum_k k n_k \right) \phi_k(T) e^{\mu k/T} \right]^{n_k} \\ &\quad \times \Theta\left(V - b \sum_k k n_k \right), \end{aligned} \tag{6}$$

where $\phi_k(T) \equiv \omega_k(T,V)/V$.

The presence of the Θ function in the GCPF (6) guarantees that only configurations with positive value of the free volume are counted. However, similarly to the delta function restriction in Eq. (5), it makes again the calculation of $\mathcal{Z}(V,T,\mu)$ (6) to be rather difficult. This problem can be solved [10] by performing the Laplace transformation of $\mathcal{Z}(V,T,\mu)$. This introduces the so-called isobaric partition function (IPF):

$$\begin{aligned} \hat{\mathcal{Z}}(s,T,\mu) &\equiv \int_0^{\infty} dV e^{-sV} \mathcal{Z}(V,T,\mu) \\ &= \int_0^{\infty} dV' e^{-sV'} \sum_{\{n_k\}} \prod_k \frac{1}{n_k!} \\ &\quad \times \{ V' \phi_k(T) e^{(\mu - sbT)k/T} \}^{n_k} \\ &= \int_0^{\infty} dV' e^{-sV'} \exp\left\{ V' \sum_{k=1}^{\infty} \phi_k e^{(\mu - sbT)k/T} \right\}. \end{aligned} \tag{7}$$

After changing the integration variable $V \to V'$, the constraint of Θ function has disappeared. Then all n_k were summed independently leading to the exponential function. Now the integration over V' in Eq. (7) can be straightforwardly done resulting in

$$\hat{\mathcal{Z}}(s,T,\mu) = \frac{1}{s - \mathcal{F}(s,T,\mu)}, \tag{8}$$

where

$$\begin{aligned} \mathcal{F}(s,T,\mu) &= \sum_{k=1}^{\infty} \phi_k \exp\left[\frac{(\mu - sbT)k}{T} \right] \\ &= \left(\frac{mT}{2\pi} \right)^{3/2} \left[z_1 \exp\left(\frac{\mu - sbT}{T} \right) \right. \\ &\quad \left. + \sum_{k=2}^{\infty} k^{3/2 - \tau} \exp\left(\frac{(\nu - sbT)k - \sigma k^{2/3}}{T} \right) \right]. \end{aligned} \tag{9}$$

Here we have introduced the shifted chemical potential $\nu \equiv \mu + W_o + T^2/\epsilon_o$. From the definition of pressure in the grand canonical ensemble

$$p(T,\mu) \equiv T \lim_{V \to \infty} \frac{\ln \mathcal{Z}(V,T,\mu)}{V}, \tag{10}$$

it follows that, in the thermodynamic limit, the GCPF of the system approaches

$$\mathcal{Z}(V,T,\mu)\big|_{V \to \infty} \sim \exp\left[\frac{p(T,\mu)V}{T} \right]. \tag{11}$$

An exponentially over V increasing part of $\mathcal{Z}(V,T,\mu)$ in the right-hand side of Eq. (11) generates the farthest-right singularity s^* of the function $\hat{\mathcal{Z}}(s,T,\mu)$, because for $s < p(T,\mu)/T$ the V-integral for $\hat{\mathcal{Z}}(s,T,\mu)$ (7) diverges at its upper limit. Therefore, in the thermodynamic limit, $V \to \infty$ the system pressure is defined by this farthest-right singularity, $s^*(T,\mu)$, of IPF $\hat{\mathcal{Z}}(s,T,\mu)$ (7) (see also Ref. [11] for more details):

$$p(T,\mu) = T s^*(T,\mu). \tag{12}$$

Note that this simple connection of the farthest-right s-singularity of $\hat{\mathcal{Z}}$, Eq. (7), to the asymptotic, $V \to \infty$, behav-

ior of $\mathcal{Z}$, Eq. (11), is a general mathematical property of the Laplace transform. Due to this property the study of the system behavior in the thermodynamic limit $V\to\infty$ can be reduced to the investigation of the singularities of $\hat{\mathcal{Z}}$.

IV. SINGULARITIES OF IPF AND PHASE TRANSITIONS

The IPF, Eq. (7), has two types of singularities.

(1) The simple pole singularity defined by the equation

$$s_g(T,\mu)=\mathcal{F}(s_g,T,\mu). \tag{13}$$

(2) The singularity of the function $\mathcal{F}(s,T,\mu)$ itself at the point s_l where the coefficient in linear over k terms in the exponent is equal to zero,

$$s_l(T,\mu)=\frac{\nu}{Tb}. \tag{14}$$

The simple pole singularity corresponds to the gaseous phase where pressure is determined from the following transcendental equation:

$$p_g(T,\mu)=\left(\frac{mT}{2\pi}\right)^{3/2}T\left[z_1\exp\left(\frac{\mu-bp_g}{T}\right)+\sum_{k=2}^{\infty}k^{3/2-\tau}\exp\left(\frac{(\nu-bp_g)k-\sigma k^{2/3}}{T}\right)\right]. \tag{15}$$

The singularity $s_l(T,\mu)$ of the function $\mathcal{F}(s,T,\mu)$ (9) defines the liquid pressure

$$p_l(T,\mu)\equiv Ts_l(T,\mu)=\frac{\nu}{b}. \tag{16}$$

In the considered model the liquid phase is represented by an infinite fragment, i.e., it corresponds to the macroscopic population of the single mode $k=\infty$. Here one can see the analogy with the Bose condensation where the macroscopic population of a single mode occurs in the momentum space.

In the (T,μ) regions where $\nu<bp_g(T,\mu)$ the gas phase dominates $(p_g>p_l)$, while the liquid phase corresponds to $\nu>bp_g(T,\mu)$. The liquid-gas phase transition occurs when two singularities coincide, i.e., $s_g(T,\mu)=s_l(T,\mu)$. A schematic view of singular points is shown in Fig. 1(a) for $T<T_c$, i.e., when $\sigma>0$. The two-phase coexistence region is therefore defined by the equation

$$p_l(T,\mu)=p_g(T,\mu),\quad \text{i.e.,}\quad \nu=bp_g(T,\mu). \tag{17}$$

One can easily see that $\mathcal{F}(s,T,\mu)$ is monotonously decreasing function of s. The necessary condition for the phase transition is that this function remains finite in its singular point $s_l=\nu/Tb$:

$$\mathcal{F}(s_l,T,\mu)<\infty. \tag{18}$$

The convergence of $\mathcal{F}$ is determined by τ and σ. At $\tau=0$ the condition (18) requires $\sigma(T)>0$. Otherwise,

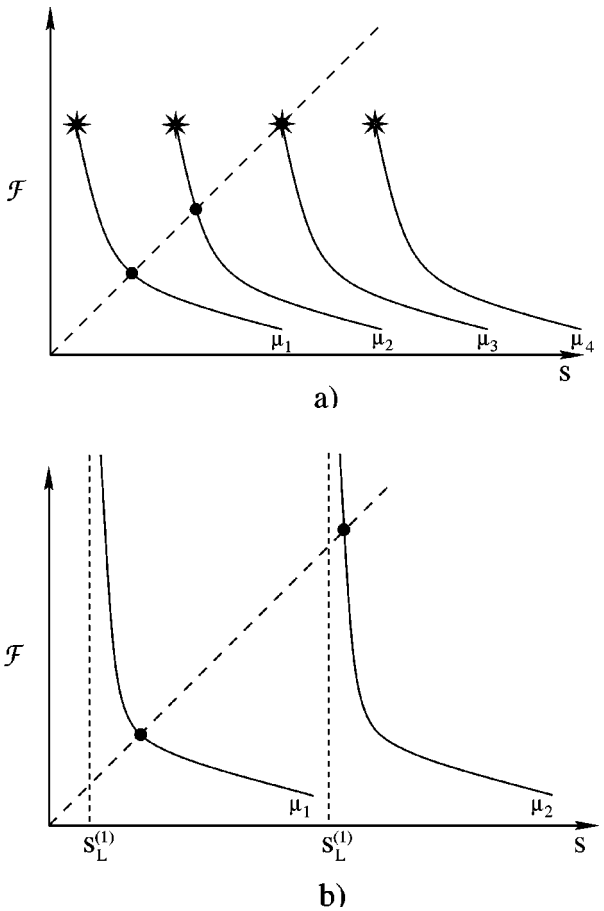

FIG. 1. Schematic view of singular points of the isobaric partition function, Eq. (8), at $T<T_c$ (a) and $T>T_c$ (b). Full lines show $\mathcal{F}(s,T,\mu)$ as a function of s at fixed T and μ, $\mu_1<\mu_2<\mu_3<\mu_4$. Dots and asterisks indicate the simple poles (s_g) and the singularity of function $\mathcal{F}$ itself (s_l). At $\mu_3=\mu^*(T)$ the two singular points coincide signaling a phase transition.

$\mathcal{F}(s_l,T,\mu)=\infty$ and the simple pole singularity $s_g(T,\mu)$ (13) is always the farthest-right s-singularity of $\hat{\mathcal{Z}}$ (7) [see Fig. 1(b)]. At $T>T_c$, where $\sigma(T)=0$, the considered system can exist only in the one-phase state. It will be shown below that for $\tau>5/2$ the condition (18) can be satisfied even at $\sigma(T)=0$.

V. FIRST ORDER PHASE TRANSITION AND MIXED PHASE

At $T<T_c$ the system undergoes the first order phase transition across the line $\mu^*=\mu^*(T)$ defined by Eq. (17). Its explicit form is given by the expression $(W\equiv W_0+T^2/\epsilon_0)$

$$\mu^*(T)=-W+\left(\frac{mT}{2\pi}\right)^{3/2}Tb\left[z_1\exp\left(-\frac{W}{T}\right)+\sum_{k=2}^{\infty}k^{3/2-\tau}\exp\left(-\frac{\sigma k^{2/3}}{T}\right)\right]. \tag{19}$$

The points on the line $\mu^*(T)$ correspond to the mixed phase states. We first consider the case when $\tau=0$. The line $\mu^*(T)$ (19) for this case is shown in Fig. 2.

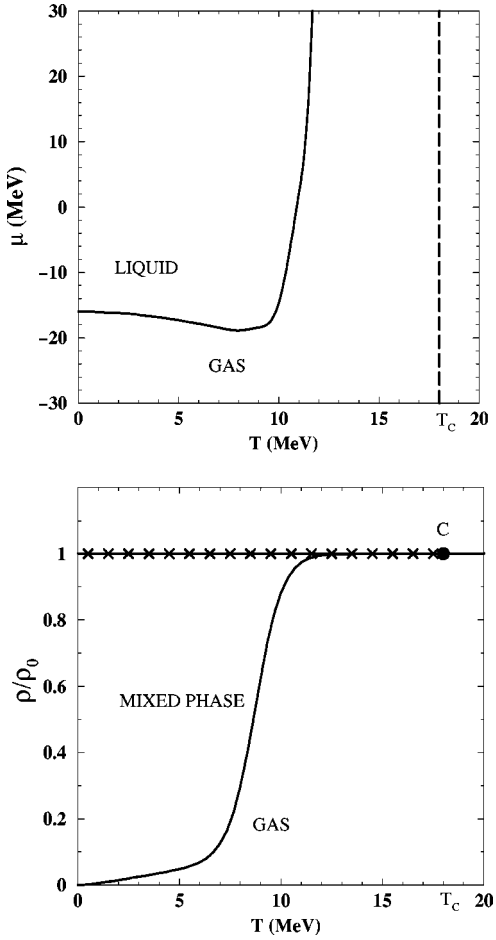

FIG. 2. Phase diagram in $T-\mu$ (upper panel) and $T-\rho$ (lower panel) planes for $\tau=0$. The mixed phase is represented by the line $\mu^*(T)$ in the upper panel and by the extended region in the lower panel. Liquid phase (shown by crosses) exists at density $\rho=\rho_0$. Point C is the critical point.

The baryonic density is calculated as $(\partial p/\partial\mu)_T$ and is given by the following formulas in the liquid and gas phases, respectively:

$$\rho_l \equiv \left(\frac{\partial p_l}{\partial \mu}\right)_T = \frac{1}{b}, \tag{20}$$

$$\rho_g \equiv \left(\frac{\partial p_g}{\partial \mu}\right)_T = \frac{\rho_{id}}{1+b\rho_{id}}, \tag{21}$$

where the function ρ_{id} is defined as

$$\rho_{id}(T,\mu) = \left(\frac{mT}{2\pi}\right)^{3/2}\left[z_1 \exp\left(\frac{\mu - bp_g}{T}\right) + \sum_{k=2}^{\infty} k^{5/2-\tau} \exp\left(\frac{(\nu - bp_g)k - \sigma k^{2/3}}{T}\right)\right]. \tag{22}$$

Due to the condition (17) this expression is simplified in the mixed phase:

$$\rho_{id}^{mix}(T) \equiv \rho_{id}(T,\mu^*(T)) = \left(\frac{mT}{2\pi}\right)^{3/2}\left[z_1 \exp\left(-\frac{W}{T}\right) + \sum_{k=2}^{\infty} k^{5/2-\tau} \exp\left(-\frac{\sigma k^{2/3}}{T}\right)\right]. \tag{23}$$

This formula clearly shows that the bulk (free) energy acts in favor of the composite fragments, but the surface term favors single nucleons.

Since at $\sigma>0$ the sum in Eq. (23) converges at any τ, ρ_{id} is finite and according to Eq. (21) $\rho_g<1/b$. Therefore, the baryonic density has a discontinuity $\Delta\rho=\rho_l-\rho_g>0$ across the line $\mu^*(T)$ (19) shown for $\tau=0$ in the upper panel of Fig. 2. The discontinuities take place also for the energy and entropy densities. The phase diagram of the system in the (T,ρ) plane is shown in lower panel of Fig. 2. The line $\mu^*(T)$ (19) corresponding to the mixed phase states is transformed into the finite region in the (T,ρ) plane. In this mixed phase region of the phase diagram the baryonic density ρ is a superposition of the liquid and gas baryonic densities:

$$\rho = \lambda\rho_l + (1-\lambda)\rho_g\,. \tag{24}$$

Here λ $(0<\lambda<1)$ is a fraction of the system volume occupied by the liquid inside the mixed phase. A similar linear combination is also valid for the energy density:

$$\varepsilon = \lambda\varepsilon_l + (1-\lambda)\varepsilon_g\,, \tag{25}$$

with $(i=l,g)$:

$$\varepsilon_i \equiv T\frac{\partial p_i}{\partial T} + \mu\frac{\partial p_i}{\partial \mu} - p_i\,. \tag{26}$$

One finds

$$\varepsilon_l = \frac{T^2/\epsilon_0 - W_0}{b}, \tag{27}$$

$$\varepsilon_g = \frac{1}{1+b\rho_{id}}\left\{\frac{3}{2}p_g + (T^2/\epsilon_0 - W_0)\rho_{id} + \left(\frac{mT}{2\pi}\right)^{3/2}\left(\sigma - T\frac{d\sigma}{dT}\right) \times\left[z_1 \exp\left(\frac{\mu - bp_g}{T}\right) + \sum_{k=2}^{\infty} k^{13/6-\tau} \times \exp\left(\frac{(\nu - bp_g)k - \sigma k^{2/3}}{T}\right)\right]\right\}. \tag{28}$$

The pressure on the phase transition line $\mu^*(T)$ (19) is a monotonously increasing function of T

$$p^*(T) \equiv p_g(T,\mu^*(T)) = \left(\frac{mT}{2\pi}\right)^{3/2} T\left[z_1 \exp\left(-\frac{W}{T}\right) + \sum_{k=2}^{\infty} k^{3/2-\tau} \exp\left(-\frac{\sigma k^{2/3}}{T}\right)\right]. \tag{29}$$

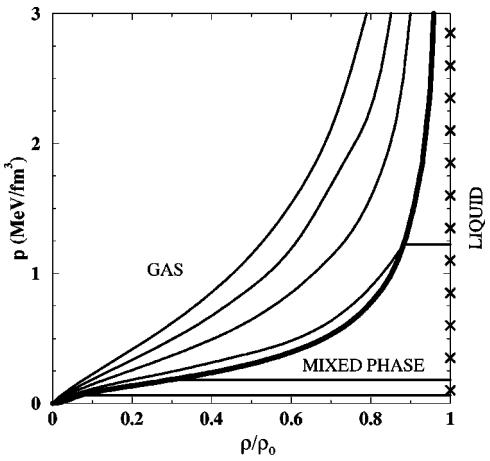

FIG. 3. Pressure isotherms (thin solid lines) as functions of reduced density ρ/ρ_o for $\tau=0$. The isotherms are shown for $T=4$, 8, 10, 14, 18, and 22 MeV from bottom to top. The boundary of the mixed and gaseous phases is shown by the thick solid line. Liquid phase is indicated by crosses. The critical point $T=T_c=18$ MeV, $\rho=\rho_o$ corresponds to infinite pressure.

Figure 3 shows the pressure isotherms as functions of the reduced density ρ/ρ_o for $\tau=0$. Inside the mixed phase the obtained pressure isotherms are horizontal straight lines in accordance with the Gibbs criterion. These straight lines go up to infinity when $T\rightarrow T_c-0$. This formally corresponds to the critical point, $T=T_c$, $\rho=\rho_c=1/b$ and $p_c=\infty$, in the considered case of $\tau=0$. For $T>T_c$ the pressure isotherms never enter into the mixed phase region. Note that, if $\sigma(T)$ would never vanish, the mixed phase would extend up to infinite temperatures.

Inside the mixed phase at constant density ρ the parameter λ is temperature dependent as shown in Fig. 4: $\lambda(T)$ drops to zero in the narrow vicinity of the boundary separating the mixed phase and the pure gaseous phase. This specific behavior of $\lambda(T)$ causes a strong increase of the energy density (25) and as its consequence a narrow peak of the specific heat $C_V(T)\equiv(\partial\varepsilon/\partial T)_\rho$. It should be emphasized

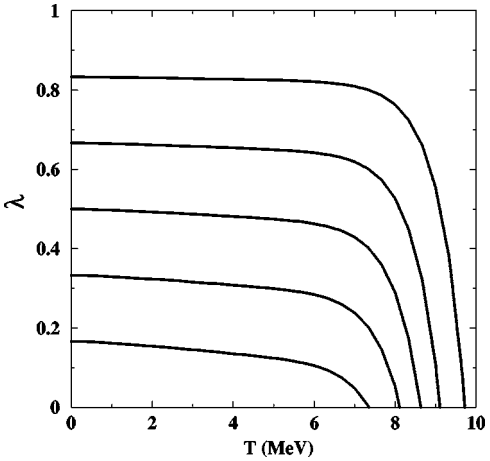

FIG. 4. Volume fraction of the liquid phase $\lambda(T)$ for $\tau=0$ shown as a function of temperature at densities $\rho/\rho_o=1/6$, 1/3, 1/2, 2/3, 5/6 (from bottom to top).

that the energy density is continuous at the boundary of the mixed phase and the gas phase, and the sharpness of the peak in C_V is entirely due to the strong temperature dependence of $\lambda(T)$ near this boundary. A narrow peak of the specific heat was observed in the canonical ensemble calculations of Refs. [6,7]. However, in contrast to the expectation in Refs. [6,7], the height of the $C_V(T)$ peak is not equal to infinity and its width is not zero in the thermodynamic limit considered in our study. Note also that the shape of the $C_V(T)$ depends strongly on the parameter τ and on the chosen value of the baryon density ρ.

VI. POSSIBILITY OF SECOND ORDER PHASE TRANSITION

The results presented in Figs. 2–4 are obtained for $\tau=0$. New possibilities appear at nonzero values of the parameter τ. At $0<\tau\leqslant 5/2$ the qualitative picture remains the same as discussed above, although there are some quantitative changes. For $\tau>5/2$ the condition (18) is also satisfied at $T>T_c$ where $\sigma(T)=0$. Therefore, the liquid-gas phase transition extends now to all temperatures. Its properties are, however, different for $\tau>7/2$ and for $\tau<7/2$ (see Fig. 5). If $\tau>7/2$ the gas density is always lower than $1/b$ as ρ_{id} is finite. Therefore, the liquid-gas transition at $T>T_c$ remains the first order phase transition with discontinuities of baryonic density, entropy, and energy densities. The pressure isotherms as functions of the reduced density ρ/ρ_o are shown for this case in Fig. 6.

At $5/2<\tau<7/2$ the baryonic density of the gas in the mixed phase, Eqs. (21) and (23), becomes equal to that of the liquid at $T>T_c$, since $\rho_{id}\rightarrow\infty$ and $\rho_g^{mix}=1/b\equiv\rho_o$. It is easy to prove that the entropy and energy densities for the liquid and gas phases are also equal to each other. There are discontinuities only in the derivatives of these densities over T and μ, i.e., $p(T,\mu)$ has discontinuities of its second derivatives. Therefore, the liquid-gas transition at $T>T_c$ for $5/2<\tau<7/2$ becomes the second order phase transition. According to standard definition, the point $T=T_c$, $\rho=1/b$ separating the first and second order transitions is the tricritical point. One can see that this point is now at a finite pressure. Figure 7 shows the pressure isotherms as functions of the reduced density ρ/ρ_o.

It is interesting to note that at $\tau>0$ the mixed phase boundary shown in Fig. 5 is not so steep a function of T as in the case $\tau=0$ presented in Fig. 3. Therefore, the peak in the specific heat discussed above becomes less pronounced.

VII. FRAGMENT MASS DISTRIBUTIONS

The density of fragments with k nucleons can be obtained by differentiating the gas pressure (15) with respect to the k-fragment chemical potential $\mu_k=k\mu$. This leads to the fragment mass distribution $P(k)$ in the gas phase

$$P_g(k)=a_o k^{3/2-\tau}\exp(-a_1 k-a_2 k^{2/3}), \qquad (30)$$

where $a_1\equiv(bp_g-\nu)/T\geqslant 0$, $a_2\equiv\sigma/T$, and a_o is the normalization constant. Since the coefficients a_o, a_1, a_2 depend on

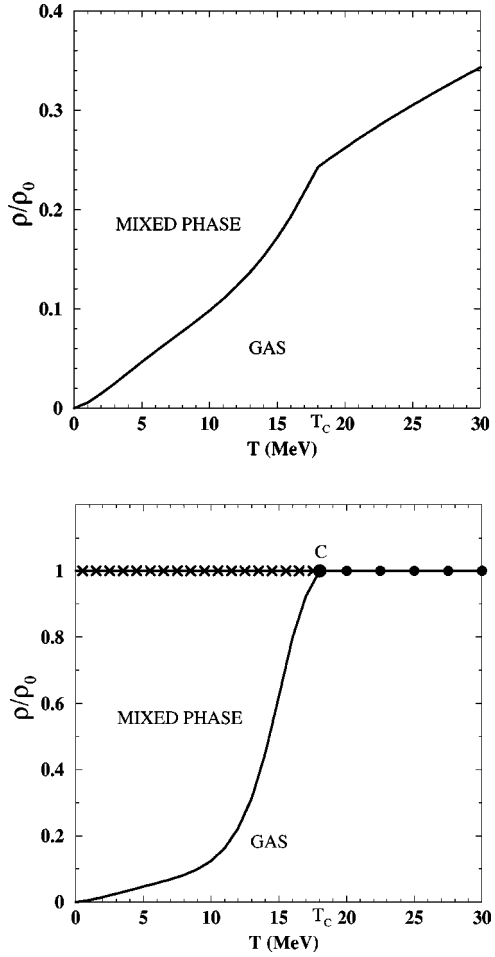

FIG. 5. Phase diagrams in $T-\rho$ plane for $\tau=3.6$ (upper panel) and $\tau=2.6$ (lower panel). Point C in the lower panel is the tricritical point. Crosses correspond to the liquid phase of the first order phase transition and dots correspond to the states of the second order one.

T and μ the distribution $P(k)$ (30) has different shapes in different points of the phase diagram. In the mixed phase the condition (17) leads to $a_1=0$ and Eq. (30) is transformed into

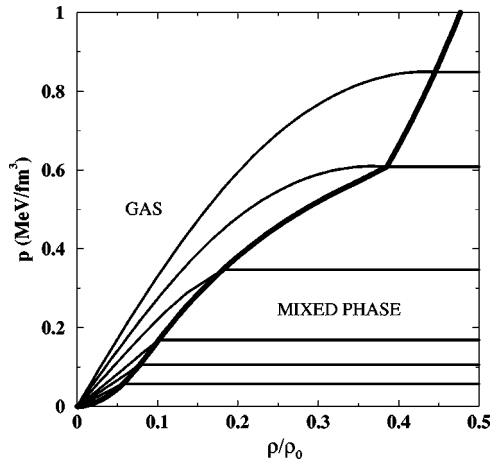

FIG. 6. The same as Fig. 3, but for $\tau=3.6$. There is no critical point in this case.

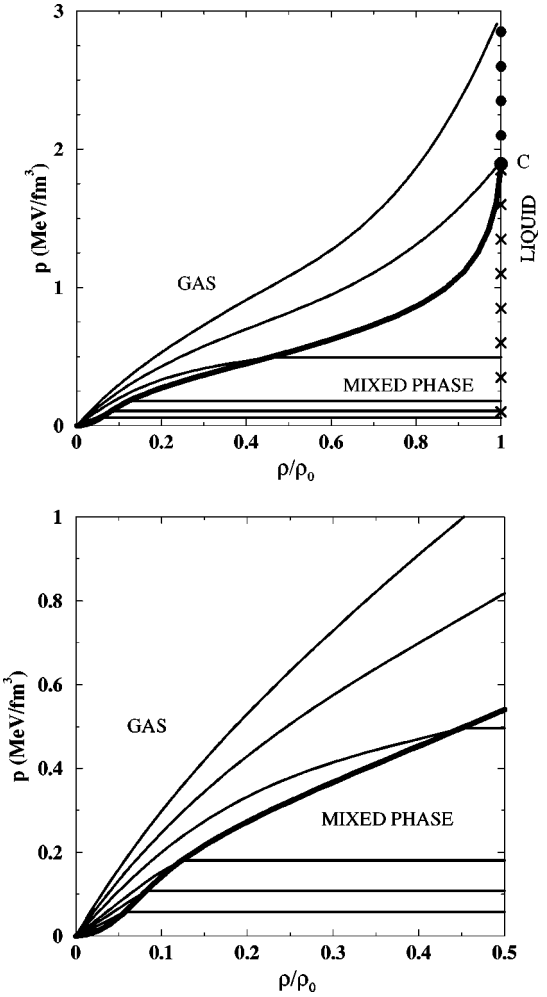

FIG. 7. The same as Fig. 3, but for $\tau=2.6$. Point C in the upper panel is the tricritical point. The lower panel differs by the scale. Crosses correspond to the liquid phase of the first order phase transition and dots correspond to the states of the second order one.

$$P_g^{mix}(k)=a_0 k^{3/2-\tau}\exp(-a_2 k^{2/3}). \tag{31}$$

The liquid inside the mixed phase is one infinite fragment which occupies a fraction λ of the total system volume. Therefore, in a large system with A nucleons in volume V $(A/V=\rho)$ the mixed phase consists of one big fragment with $\lambda V\rho_0$ nucleons (liquid) and $(1-\lambda)V\rho_g$ nucleons distributed in different k-fragments according to Eq. (31) (gas). At low T most nucleons are inside one big liquid-fragment with only few small gas fragments distributed according to Eq. (31) with large a_2. At increasing temperature the fraction of the gas fragments increases and their mass distribution becomes broader since $a_2(T)$ in Eq. (31) decreases. Outside the mixed phase region the liquid disappears and the fragment mass distribution acquires an exponential falloff, Eq. (30). Therefore, the fragment mass distribution is widest at the boundary of the mixed phase. At even higher temperatures, $T>T_c$, the coefficient a_2 vanishes.

Details of the fragment mass distribution depend on the parameter τ. At $\tau<5/2$ we observe a sudden transformation of the large liquid fragment into light and intermediate mass fragments in the narrow vicinity of the mixed phase bound-

ary. This sudden change of the fragment composition has the same origin as a narrow peak in the specific heat, i.e., a sharp drop of $\lambda(T)$ near the mixed phase boundary (see Fig. 4). For larger τ all these changes are getting smoother.

An interesting possibility opens when $5/2<\tau<7/2$. As shown in Fig. 7 the mixed phase in this case ends at the tricritical point $T=T_c$, $\rho=\rho_o$. In this point both the coefficients a_1 and a_2 vanish and the mass distribution becomes a pure power law

$$P_g(k)=a_o k^{3/2-\tau}. \tag{32}$$

At $\tau>7/2$ the mixed phase exists at all T. Thus the mass distribution of gaseous fragments inside the mixed phase fulfills a power law (32) at all $T>T_c$.

VIII. CONCLUSIONS

We have used a simplified version of the statistical multifragmentation model (SMM) [1] to establish the relationship between multifragmentation phenomenon and a liquid-gas phase transition in nuclear matter. Recently, in Refs. [6,7] interesting peculiarities of this model were found numerically in the canonical ensemble formulation. In present paper this simplified SMM is solved analytically by considering the thermodynamic limit $V\to\infty$ in the grand canonical ensemble. The progress has been achieved by applying an elegant mathematical method which reduces the description of phase transitions to the investigation of singularities of the isobaric partition function. In this way we have exactly solved the model in the thermodynamic limit. The excluded volume effects are fully taken into account.

The model clearly demonstrates the first order phase transition of the liquid-gas type. It is rather surprising that in thermodynamic limit the liquid phase emerges as an infinite-mass fragment. The structure of the mixed phase and some peculiar properties near its boundary are discussed in details. The phase diagram appears to be rather sensitive to the value of the parameter τ in the Fisher's free energy term included in our treatment. New interesting possibilities for the phase diagram emerge for $\tau>5/2$ in comparison with the case when $\tau<5/2$. The case $5/2<\tau<7/2$ is particularly interesting because of the appearance of the tricritical point separating the first and second order phase transitions.

The results presented in this paper will be further developed taking into account additional physical inputs (e.g., finite size effects, Coulomb interactions and symmetry energy) to make the model closer to reality.

ACKNOWLEDGMENTS

The authors gratefully acknowledge the warm hospitality of the Institute for Theoretical Physics of the Frankfurt University. K.A.B. and I.N.M. are grateful to the Alexander von Humboldt Foundation for financial support. M.I.G. acknowledges financial support of DFG, Germany.

[1] J.P. Bondorf, A.S. Botvina, A.S. Iljinov, I.N. Mishustin, and K.S. Sneppen, Phys. Rep. **257**, 131 (1995).
[2] D.H.E. Gross, Phys. Rep. **279**, 119 (1997).
[3] A.S. Botvina *et al.*, Nucl. Phys. **A584**, 737 (1995).
[4] M. D'Agostino *et al.*, Phys. Lett. B **371**, 175 (1996); Nucl. Phys. **A560**, 329 (1999).
[5] J. Pochodzalla *et al.*, Phys. Rev. Lett. **75**, 1040 (1995).
[6] S. Das Gupta and A.Z. Mekjian, Phys. Rev. C **57**, 1361 (1998).
[7] S. Das Gupta, A. Majumder, S. Pratt, and A. Mekjian, nucl-th/9903007.
[8] K.C. Chase and A.Z. Mekjian, Phys. Rev. C **52**, R2339 (1995).
[9] M.E. Fisher, Physics **3**, 255 (1967).
[10] M.I. Gorenstein, V.K. Petrov, and G.M. Zinovjev, Phys. Lett. **106B**, 327 (1981).
[11] M.I. Gorenstein, W. Greiner, and S.N. Yang, J. Phys. G **24**, 725 (1998).